

## NMR test of McMillan's concept of discommensurations in $2H$ -TaSe<sub>2</sub>

B. H. Suits, S. Couturié,\* and C. P. Slichter

*Physics Department and Materials Research Center, University of Illinois, Urbana, Illinois 61801*

(Received 3 December 1980)

We have studied the <sup>77</sup>Se NMR in a single-crystal sample of  $2H$ -TaSe<sub>2</sub> to test McMillan's proposal regarding incommensurate charge-density waves (CDW). We compare the temperature dependence of the NMR line shape from 4.2 to 130 K with predictions based on McMillan's proposal and the theory which preceded McMillan's proposal. We confirm McMillan's hypothesis of "discommensurations"—that the incommensurate CDW is best described by commensurate regions separated by regions of phase slip. In addition we derive amplitude and phase information for the commensurate and incommensurate CDW in  $2H$ -TaSe<sub>2</sub> and make a detailed comparison with the neutron-diffraction results of Moncton *et al.* We also find a change in the phase angle of the CDW at a Ta site between 30 and 60 K and an anomaly in the sample resistance near 40 K.

### I. INTRODUCTION

In an ordinary metal the conduction-electron density is uniform from one lattice site to another. Some metals, in particular the  $2H$  polytype of TaSe<sub>2</sub>, have anomalous properties which have been attributed to a static modulation in the conduction-electron density which may have a periodicity determined in part by the Fermi surface rather than the underlying crystal lattice.<sup>1,2</sup> This modulation is called a charge-density wave (CDW) and it is accompanied by a periodic lattice distortion (PLD).

At high temperatures (> 122 K)  $2H$ -TaSe<sub>2</sub> appears to be an ordinary metal. At low temperatures, x-ray,<sup>3</sup> electron,<sup>1</sup> and neutron<sup>4</sup> diffraction studies show that a PLD, and hence a CDW, is present with a periodicity which spans an integer number of unit cells. This is the so-called commensurate state and is described by the sum of three plane waves, each with a wavelength equal to three lattice constants. Raman studies show that the modulation of the "normal" conduction-electron density has the hexagonal symmetry of the host lattice.<sup>5</sup> Lattice displacements have been derived for the commensurate CDW (Refs. 4 and 5), however, there have been theoretical arguments which suggest they are in error by a minus sign.<sup>6,7</sup>

At intermediate temperatures (90–122 K) the periodicity of the modulation spans a nonintegral number of unit cells. This is the so-called incommensurate state. The incommensurate state in  $2H$ -TaSe<sub>2</sub> has been usually described as the sum of three plane waves, each of which has a periodicity which is almost, but not exactly, equal to three lattice spacings. We label this model the conventional incommensurate model. McMillan,<sup>8</sup> using calculations employing a Landau model, has proposed that in the incommensurate temperature region the CDW can be better described as having regions which have the periodicity of the commensurate wave separated by "phase-slip" regions or "discommensurations."

The difference in wavelengths between the incommensurate and commensurate states is then related to the density of discommensurations. Thus, the McMillan incommensurate state involves a large portion of  $k$  space in contrast to the conventional model which is described in terms of a small number of plane waves. Nakanishi and Shiba<sup>9</sup> have extended McMillan's model and show that these discommensurations can appear as a dislocation lattice in an otherwise commensurate CDW lattice. The theory of the domain-wall interactions has been developed in some detail by Bak, Mukamel, Villain, and Wentowska.<sup>10</sup>

Discrete regions of phase slip in an otherwise commensurate structure were first discussed to describe dislocations in one-dimensional systems by Frank and van der Merwe.<sup>11</sup> Domains of commensurate structure in an otherwise incommensurate state have been observed using magnetic resonance by Moskalev, Belobrova, and Aleksandrova<sup>12</sup> in the modulated dielectric Rb<sub>2</sub>ZnCl<sub>4</sub>, by Fukui, Sumi, Hatta, and Abe in organic compound TSHD,<sup>13</sup> and by Chaves, Gazzinelli, and Blinc in K<sub>2</sub>SeO<sub>4</sub>.<sup>14</sup> Blinc *et al.*<sup>15,16</sup> also studied Rb<sub>2</sub>ZnCl<sub>4</sub> with magnetic resonance. They found a fraction of commensurate-like structures in the incommensurate state which was very small (~1%) except very near the incommensurate-commensurate transition where the fraction goes continuously to 1.

The first evidence for the McMillan incommensurate CDW state was an anomalously large harmonic observed in the neutron diffraction study of Moncton *et al.*,<sup>4</sup> which they related to the third-order ("lock-in") term in a free-energy expansion. It has also been suggested<sup>17</sup> that the NMR results obtained by Berthier *et al.*<sup>18</sup> indicate the presence of a tendency towards commensurate regions with-

in the incommensurate state of NbSe<sub>2</sub>. However, since NbSe<sub>2</sub> exhibited no commensurate CDW, a direct comparison between the incommensurate and commensurate states was not possible.

Since the NMR frequency of a nucleus in a metal is strongly dependent on the conduction-electron density at or near the nucleus, NMR provides a microscopic (real-space) probe of the CDW. One can use simple qualitative arguments to relate the CDW to the PLD observed by diffraction techniques.

In this paper we report a detailed NMR line-shape study of the <sup>77</sup>Se nuclear magnetic resonance in a single-crystal sample of 2H-TaSe<sub>2</sub>. For the incommensurate temperature region we use McMillan's theory to calculate line shapes and show that his proposal appears correct. Some of our arguments were presented in a previous paper.<sup>19</sup> In the commensurate region we show line shapes which support the theoretical arguments that the low-temperature atomic displacements obtained from the neutron diffraction data are indeed in error. We also show that it is possible that the atomic displacements change between onset (90 K) and low temperatures (4.2 K).

## II. GENERAL DESCRIPTION OF THE CDW

For the sake of clarity we describe our choice of coordinates and nomenclature at the outset. Since 2H-TaSe<sub>2</sub> is a layered structure with a small interlayer coupling, we restrict our description to one layer assuming that the contribution to our NMR signal is the same for all other layers. The symmetry of the crystal and results of previous investigations show that this assumption is valid.<sup>4,5</sup> Figure 1 shows a section of one layer projected onto a plane and defines the coordinate system used throughout the rest of this paper.

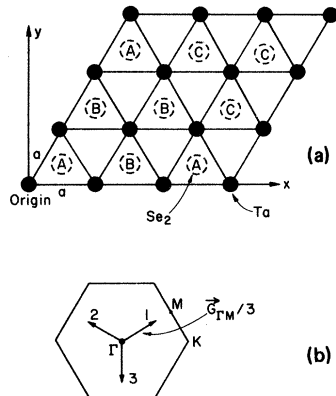


FIG. 1. (a) Section of one layer of 2H-TaSe<sub>2</sub> showing the coordinate system used throughout this paper. (b) First Brillouin zone showing the directions of the wave vectors used.

Holy *et al.*<sup>5</sup> showed that the PLD, and by extension the CDW, has hexagonal symmetry. Thus we write the charge density,  $\rho(\vec{r})$ , in terms of the normal charge density,  $\rho_0(\vec{r})$ , as

$$\rho(\vec{r}) = \rho_0(\vec{r})[1 + \alpha(\vec{r})], \quad (1)$$

where  $\alpha(\vec{r})$  can be written as a Fourier series, each term having the symmetry of the lattice. We write the first term in this series as

$$\alpha_1(\vec{r}) = A_1 \text{Re} \sum_{j=1}^3 \exp(i\vec{q}_j \cdot \vec{r} + i\phi_j), \quad (2)$$

where the sum is over the three wave vectors in the  $\Gamma M$  directions as shown in Fig. 1. Experiment shows that the length of the wave vectors in the commensurate state should be taken to be exactly one-third of the reciprocal-lattice vector in the  $\Gamma M$  direction.<sup>1,3,4</sup> For the conventional incommensurate state we would place  $\vec{q}_j = \vec{G}_{\Gamma M}(1 - \delta)/3$ , where  $\delta$  is typically between 1% and 2%. The McMillan incommensurate state is more complicated. In this case one takes the  $\vec{q}_j$  to be the commensurate wave vectors with the origin of the  $\vec{r}$ 's translated by one lattice spacing as one crosses a discommensuration. The parameter  $\delta$  then describes the average deviation from the commensurate wave vector and has been carefully measured by Fleming *et al.*<sup>3</sup>

## III. KNIGHT SHIFT WITH A CDW PRESENT

The Knight shift of the NMR signal from a nucleus at  $\vec{R}_i$  in an applied field  $H_0$  due to *s*-like conduction electrons can be written<sup>20</sup>

$$K(\vec{R}_i) \equiv \frac{\Delta H}{H_0} = \frac{8\pi}{3} \sum_k |\psi_k(\vec{R}_i)|^2 \chi_k^s, \quad (3)$$

where  $|\psi_k(\vec{R}_i)|^2$  is the square of the electronic wave function at  $\vec{R}_i$  and  $\chi_k^s$  is the contribution to the total electronic spin susceptibility from the electronic state characterized by the index  $k$ . The total electronic density is of course given by

$$\rho(\vec{R}) = \sum_k |\psi_k(\vec{R})|^2 f(k), \quad (4)$$

where  $f(k)$  is the probability that the state  $k$  is occupied.

In a noninteracting free-electron model,  $\chi_k^s$  from states away from the Fermi surface is negligible and the contribution from each state at the Fermi surface is essentially equal. If we introduce a periodic distortion characterized by a wave vector which spans (or almost spans) the Fermi surface, a band gap will open at the Fermi surface and those states at the gap no longer contribute to the sum in Eq. (3). In addition, to first order in the perturbing potential, we have a spatial modulation

of the wave function squared with the same periodicity and phase as the perturbing potential.

The Knight shift is related to the wave function squared, summed over states at the Fermi surface (away from any gaps), whereas the total conduction-electron density is given by the sum of all occupied states. In the noninteracting free-electron model the spatial changes in the conduction-electron density when a small perturbation is introduced are proportional to the spatial variations of the Knight shift given by Eq. (3). Interactions other than that given by Eq. (3) which may be present, such as an orbital contribution, would behave like a weighted average of the total occupied electron density. That is, the spatial changes in the interaction would be between those of Eqs. (3) and (4), and hence would also be linearly related to the conduction-electron density for small perturbation. Since the atomic motions in  $2H\text{-TaSe}_2$  are about 1% of the lattice constants<sup>4</sup> we can hope that we are in the small perturbation limit and the spatial variations of the Knight shift are, within the free-electron model, linearly related to the CDW and PLD. Of course, the rather complicated band structure of  $2H\text{-TaSe}_2$  and the possibility of interband mixing complicates the present situation so that the applicability of the systematics derived from the noninteracting free-electron model is not clear. However, at least qualitatively, we expect the changes in the Knight shift to reflect the changes in the potential in  $2H\text{-TaSe}_2$  in this simple linear fashion.

We will look at the change in the average wave function as it manifests itself in the NMR line shape. Changes in the susceptibility,  $\chi_k^s$ , would presumably be the same at all  $^{77}\text{Se}$  sites.

The contribution to the total NMR signal of a nucleus at  $\vec{R}_i$  will be given by a line-shape function  $g(\omega - \omega_i)$ , centered at a frequency,  $\omega_i$ , shifted by  $\gamma H_0 K(\vec{R}_i)$  from the "free-nuclear" frequency, where  $\gamma$  is the gyromagnetic ratio. Quite generally

we can expect  $K(\vec{R}_i)$  to have the same periodicity as the charge density given by Eq. (2). That is, we write

$$K(\vec{R}_i) = K_0(T) + K_1(T) \text{Re} \sum_{j=1}^3 \exp(i\vec{q}_j \cdot \vec{R}_i + i\theta_j) \quad (5)$$

+ higher harmonics,

where  $K_0$  represents the contribution which is the same for all nuclei but may be a function of temperature  $T$ ,  $K_1$  is the amplitude of the modulation of the first harmonic, and the  $\vec{q}_j$  are the same as those used in Eq. (2). If the origin is taken as a Ta site, then in the commensurate state there are three distinct Se sites (labeled A, B, and C in Fig. 1) which occur with equal numbers. Thus, we expect three NMR lines with equal intensities. To obtain a unique parametrization we must then drop all higher-order terms in Eq. (5). One must keep in mind that higher harmonics may be present though not discernible. The phase angle  $\theta_0$  determines the relative spacings of the three NMR lines. This is shown in Fig. 2.

For the case of the incommensurate CDW we have adopted a slightly different formalism which

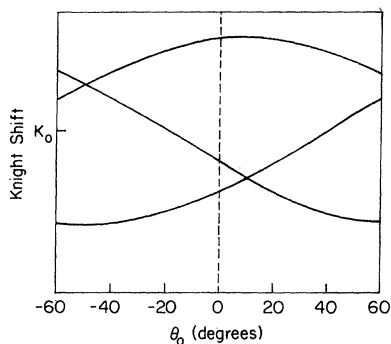


FIG. 2. Spacing of the three  $^{77}\text{Se}$  NMR lines as a function of the phase angle  $\theta_0$ .

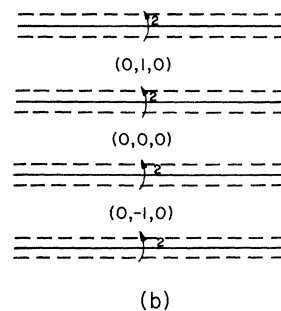
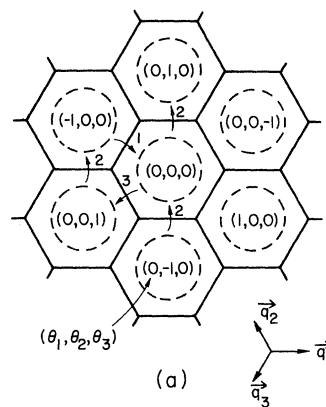


FIG. 3. Hexagonal (a) and striped (b) incommensurate structures. The numbered arrows indicate which of the phase angles defined by Eq. (6) change across a discommensuration. Angles are in units of  $2\pi/3$ .

has the flexibility that by adjusting one parameter one can obtain the NMR line shape corresponding to a conventional incommensurate, a McMillan incommensurate, or a commensurate line shape. We start by rewriting Eq. (5) following the results of Nakanishi and Shiba<sup>9</sup> in the form

$$K(\vec{R}_i) = K_0(T) + K_1(T) \sum_{j=1}^3 \cos[\vec{q}_j \cdot \vec{R}_i + \theta_j(\vec{R}_i) - \theta_{j+1}(\vec{R}_i) + \theta_0], \quad (6)$$

where  $\theta_4 = \theta_1$  and the  $\vec{q}_j$ 's are the commensurate wave vectors shown in Fig. 1. One then distinguishes the different types of models by the dependence of the  $\theta_j$ 's on the  $\vec{R}_i$ 's.

For the commensurate state the  $\theta_j$ 's are all zero. Fleming *et al.*<sup>3</sup> observed two types of incommensurate phases: one consistent with a hexagonal structure, the other with a striped structure. We illustrate how the phase angles  $\theta_j$  change for these two structures in Fig. 3. Note that a change of  $\theta_2$  by  $2\pi/3$  is equivalent to a simultaneous change of  $\theta_1$  and  $\theta_3$  by  $-2\pi/3$ .

To calculate the total NMR signal we need to sum over all  $\vec{R}_i$ 's. It is simpler, yet equivalent, to fix  $\vec{R}_i$  and sum over the  $\theta_j$ 's with a weighting function  $\eta(\theta_j)d\theta_j$ , which corresponds to how often a particular  $\theta_j$  occurs throughout all the  $R_i$ 's. To calculate  $\eta(\theta)$  we take the differential equation which McMillan derived assuming only phase modulation is important and integrate once to obtain

$$\eta(\theta) \propto \alpha \left( \frac{dx}{d\theta} \right) = \left[ \sin^2 \left( \frac{3\theta}{2} \right) + \gamma^2 \right]^{-1/2}, \quad (7)$$

where  $\alpha$  is defined by McMillan and is proportional to the square root of the magnitude of the CDW and  $\gamma^2$  is an integration constant. To illustrate the significance of  $\gamma$  we show  $\theta(x)$  as a function of  $\alpha x$  for several values of  $\gamma$  in Fig. 4. As  $\theta(x)$  changes by  $2\pi/3$  the origin of the CDW appears to move from one Ta site to a nearest-neighbor site. It can be seen that  $\gamma$  gives a measure of the width

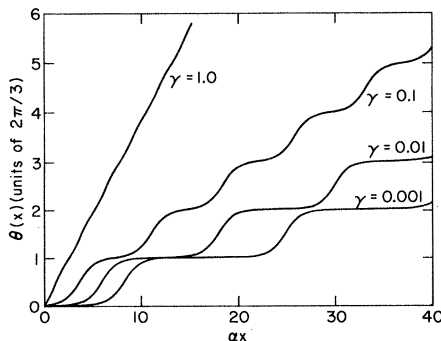


FIG. 4. Phase angle  $\theta(x)$  as a function of  $\alpha x$  and  $\gamma$  according to McMillan's theory.

of the "phase-slip" region compared to the distance between phase slips. McMillan's parameter  $\delta$  can then be related to our  $\gamma$  in terms of  $\alpha$  and elliptic integrals.

The limiting cases are the following:

- (i)  $\gamma \rightarrow 0$ , commensurate  $\eta(\theta) \rightarrow \delta(\theta)$ , and
- (ii)  $\gamma \rightarrow \infty$ , conventional incommensurate  $\eta(\theta) \rightarrow \text{constant}$ .

McMillan's incommensurate state would then be a situation between (i) and (ii). We approximate the three-phase angle density function by the product of three single-phase density functions. This should be a better approximation for the hexagonal incommensurate structure than for the striped structure.

We can now compute the total NMR signal from the Knight-shift equations by calculating the frequency of the NMR signal for each set of  $\theta_j$ 's and summing over all sets. We then broaden the resulting line shape with a Lorentzian function and normalize it. Ideally, the experimental data are derivatives of the true NMR absorption signal. In practice the signal is distorted due to the long-time constant filtering and large modulation amplitudes necessary to increase the signal-to-noise ratio to an acceptable level. Wind and Emid<sup>21</sup> have developed a formalism to remove the experimental distortion from the data. However, we found that it was much more reliable to put the modulation and filter distortions into our theoretical line shapes to obtain pseudoexperimental spectra which may then be compared directly to the data. To be specific, the pseudoexperimental derivative signal  $s(x)$  is related to the undistorted line shape  $f(x)$  by

$$s(x) = F^{-1} \left( \frac{-2iJ_1(x_m u)}{(1 - iux_{RC})^2} F(f(x)) \right), \quad (8)$$

where  $F$  is a Fourier transform,  $J_1$  is a Bessel function,  $u$  is the transform variable,  $x_m$  is the magnetic field modulation amplitude, and  $x_{RC}$  is the lock-in amplifier's  $RC$  time constant (12 dB/octave). Computed spectra for  $\theta_0 = 0^\circ$  and for several values of  $\gamma$  are shown in Fig. 5.

## IV. EXPERIMENTAL

### A. General considerations

A single crystal was used to avoid the ambiguity that arises when interpreting spectra from powders. Although NMR of a metallic single crystal has far less sensitivity than that of a powder due to the attenuation of rf fields in the bulk metal caused by the skin depth effect, in a powder all possible crystal orientations are present, causing an averaging out of spectral details. In particular, the Knight shift becomes hard to interpret, having

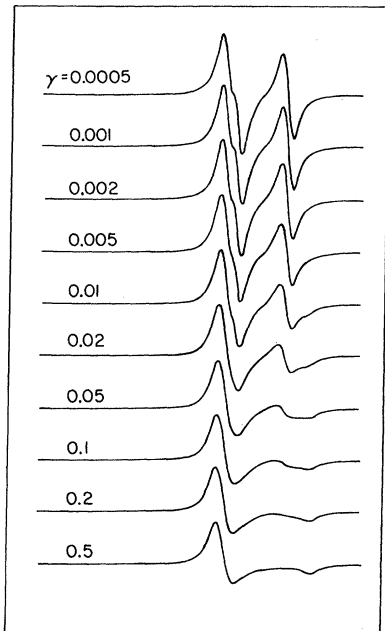


FIG. 5. Simulated NMR derivative absorption spectra based on three Lorentzians and McMillan's theory.

isotropic and anisotropic components. Using a single crystal removes these problems and makes the analysis of the data in the incommensurate phase more straightforward.

One can, in principle, observe either the  $^{181}\text{Ta}$  or the  $^{77}\text{Se}$  NMR spectra.  $^{181}\text{Ta}$  ( $I = \frac{7}{2}$ ) is 100% abundant but has a very large quadrupole moment. We could not see the  $^{181}\text{Ta}$  resonance in our single-crystal sample presumably since the NMR line is very broad due to strains in the crystal.  $^{77}\text{Se}$  ( $I = \frac{1}{2}$ ) has the disadvantage that it is only 7.5% abundant. We found the  $^{77}\text{Se}$  NMR signal to be very weak but observable.

#### B. Sample

The sample used in this study was about  $1 \text{ cm}^2$  by  $0.05 \text{ cm}$  thick, weighing about 350 mg. It was grown using iodine vapor transport by S. Meyer. The polytype of the sample was verified using single-crystal x-ray diffraction. We measured the residual resistance ratio for this sample to be  $R(295 \text{ K})/R(4.2 \text{ K}) = 88 \pm 2$ .

Since it has been suggested that the commensurate-incommensurate transition temperatures for these samples are highly sample dependent, Suits and Chen<sup>22</sup> performed precision electrical resistance measurements on our NMR sample. They saw transitions at about 90 and 120 K on heating and cooling and a transition at about 110 to 112 K which occurred only on the heating cycle. Figure 6 shows the derivative of the sample re-

sistance as a function of temperature obtained by Suits and Chen. The bump around 90 K corresponds to the incommensurate-commensurate transition and the dip around 120 K is the normal-incommensurate transition. The small bump between about 110 and 112 K which occurs only on heating is associated with an incommensurate-incommensurate transition. Their results are in excellent agreement with the results of Fleming *et al.*<sup>3</sup> The similarity between the hysteresis in the resistance presented by Suits and Chen and the hysteresis in the average incommensurate wave vector seen by Fleming *et al.* is unmistakable. We can conclude that the commensurate-incommensurate transition temperature is about 90 K and the sample is in an incommensurate state between 90 and 120 K.

#### C. NMR measurements

The nuclear magnetic resonance spectrometer used for this study was essentially that used by Abbas, Aton, and Slichter<sup>23</sup>: a phase-coherent bridge system using field modulation, lock-in detection, and signal averaging to increase the signal-to-noise ratio of the weak resonances studied. A Westinghouse superconducting solenoid was used to produce the 50-kG dc magnetic field used in these measurements.

A copper coil was wrapped directly on the sample in order to maximize the filling factor. Stakelon<sup>24</sup> has shown that for a bulk metallic sam-

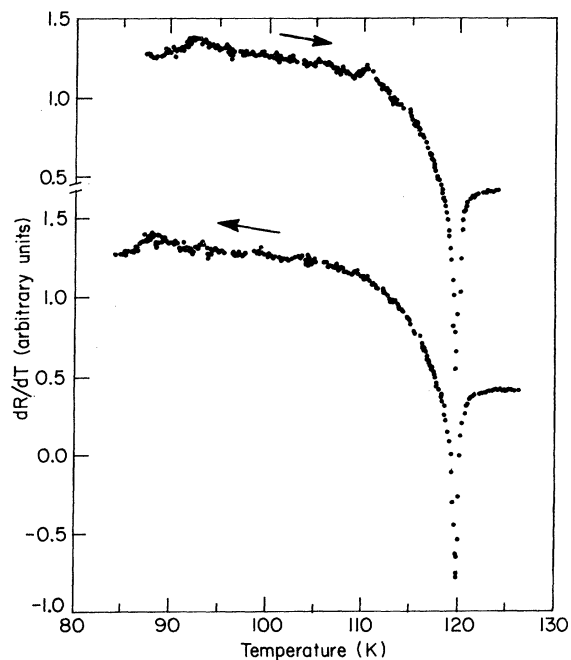


FIG. 6. Derivative of the sample resistance as a function of temperature (from Ref. 15).

ple this method gives optimum signal-to-noise ratio. The crystal was coated with varnish to help prevent shorts to the sample.

With a phase-coherent bridge system, any ratio-frequency phase can be selected for detection and study. It is most useful, however, to study the resonance with the phase set for absorption. Because the TaSe<sub>2</sub> crystal is a metal with a thickness greater than two skin depths, the well known phenomenon of mode mixing<sup>25</sup> occurs. The rf phase in our experiments was set by observing the <sup>63</sup>Cu line of the copper wire in the coil itself. The signal-to-noise ratio of the <sup>63</sup>Cu NMR is large enough to permit easy observation with a single sweep of the magnetic field.

The <sup>77</sup>Se resonance from the sample, however, is much weaker. In order to obtain sufficient signal-to-noise ratio the signal was accumulated in a digital signal averager. The number of sweeps required for a signal-to-noise ratio of 10 or more ranged from 1000 at 4.2 K to about 4000 at 100 K, taking as long as 36 h per spectrum.

The temperature-control system was stable to 0.3 K over 8 h. Over shorter periods, the system could be stable to 0.1 K. Temperature measure-

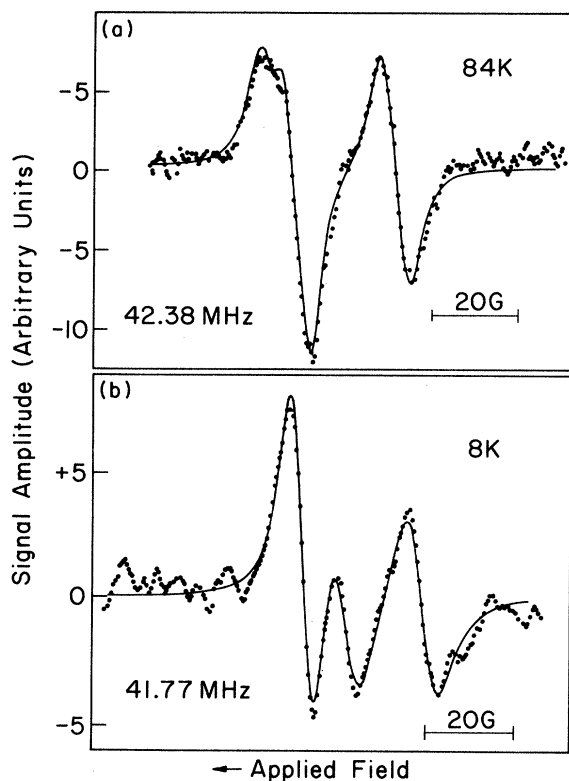


FIG. 7. NMR spectra near onset (a) and at low temperatures (b) showing the change in line positions. The theoretical curve (solid lines) is based on the sum of three Lorentzians with equal areas.

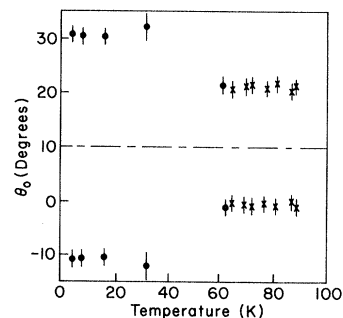


FIG. 8.  $\theta_0$  as obtained from fits similar to those in Fig. 5. At each temperature there are two possible values which are spaced symmetrically about 10°.

ments were made with a GaAs diode. The diode was calibrated by comparison with an Au-0.7% Fe-Chromel thermocouple at zero magnetic field. The correction in the diode's temperature measurements due to high magnetic fields was estimated to be 0.9 K.

## V. RESULTS

### A. Commensurate

Figure 7 shows two representative NMR absorption spectra taken below 90 K. The theoretical curve is simply the sum of three Lorentzians with equal areas. The experimental derivative is generated as described earlier.

Figure 8 and the left-hand side of Fig. 9 show the results of least-squares fit to our data below 90 K. From Fig. 2, there are two possible values of  $\theta_0$  which can describe the CDW near 90 K and two different values near 4.2 K. We will discuss this in more detail in Sec. VI.

### B. Incommensurate

Figure 10 shows several of our NMR spectra taken sequentially on a cooling cycle. The evolu-

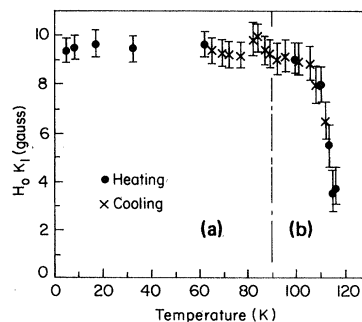


FIG. 9. Amplitude of the Knight-shift modulation as a function of temperature obtained from least-squares fits. The fits on the left (a) are based on three Lorentzians with equal areas while those on the right (b) include McMillan's discommensurations.

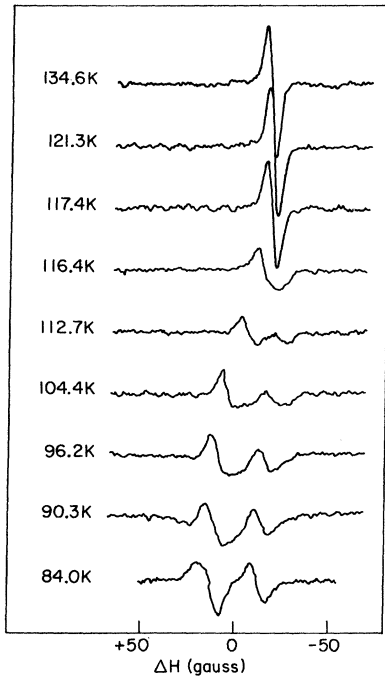


FIG. 10. NMR spectra on a cooling cycle showing the relatively gradual change from a single line at high temperature to three lines below 90 K.

tion from the single line above 120 K to the commensurate state is seen to be gradual. This is consistent with McMillan's incommensurate state,

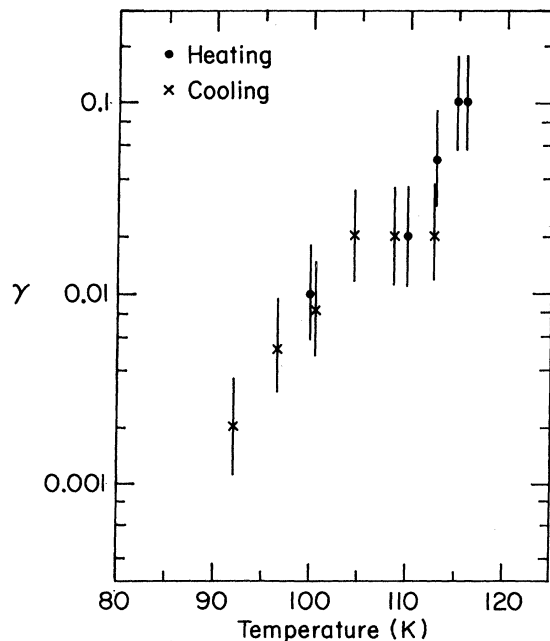


FIG. 11. Parameter  $\gamma$  as a function of temperature from fits to the data. The error bars represent the statistical errors of the fits.

where one expects the commensurate regions of the incommensurate state to yield the same three-line pattern as the commensurate state. Figure 11 and the right-hand side of Fig. 9 show the results of fits to our data using the incommensurate model described earlier. For these fits we have taken  $\theta_0 = 0$  though the line shape is not very sensitive to variations. In particular,  $\theta_0 = 20^\circ$  gives results noticeably, but not significantly, different.

The origin of the slight increase in the Knight shift as one approaches the normal-incommensurate transition from above is unknown. One possibility is that second-order terms in  $|\psi(\vec{R}_i)|^2$  are present which do not average to zero in the presence of fluctuations.

## VI. DISCUSSION

### A. Commensurate

The first thing to note regarding the commensurate spectra is that they are described very well by three lines with equal intensity. Secondly, by considering Fig. 2, the line splittings for the high-temperature region corresponds to a phase angle  $\theta_0$  of either  $0^\circ$  or  $20^\circ$  and in the low-temperature region to  $-10^\circ$  or  $30^\circ$ .

If we consider a simple model where the lattice displacements go like the gradient of the charge density which goes like our Knight-shift expansion [Eqs. (2)–(5)], then we can estimate the directions of the displacements. The displacements for our experimental values of  $\theta_0$  are illustrated in Fig. 12. We note that the displacements given by Moncton *et al.* at 5 K are not consistent with the any of the four possibilities. However,  $\theta_0 = 0$  is consistent with the NMR results of Berthier *et al.*<sup>18</sup> for  $\text{NbSe}_2$ , the Mössbauer data of Pfeiffer, Eibschütz,

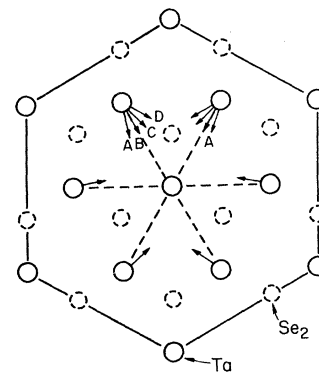


FIG. 12. Direction of the displacements calculated for the two possible low-temperature phase angles (A and D) and the two possible high-temperature commensurate phase angles (B and C). For clarity only the A displacements are shown for all Ta atoms, the rest may be obtained by symmetry.

and Salomon<sup>26</sup> for  $1T$ -TaSe<sub>2</sub>, and the suggestion<sup>6,7</sup> that the displacements presented by Moncton *et al.* are in error by a minus sign.

The change in  $\theta_0$  between 30 and 60 K has not been seen before and may be related to the change in the Raman spectra seen by Holy *et al.*<sup>5</sup> around 30 K and the anomalous low-temperature behavior in the Hall coefficient reported by Lee *et al.*<sup>27</sup> A changing phase angle has been considered by McMillan.<sup>8</sup> He shows that the phase angle may be determined by a CDW interlayer interaction and derives a relation between the amplitude of the CDW and its phase. Since  $K_1$  appears constant for the entire commensurate temperature region we conclude that McMillan's mechanism cannot be responsible for the change we observe. This does not rule out the possibility that the phase change is related to the double Fermi-surface characteristic of the  $2H$  polytypes.<sup>28</sup> We note also that the inclusion of the next (nonconstant) term in our expansion of the Knight shift [Eq. (5)] could also cause an apparent phase-angle change in our NMR spectra and would complicate any comparison with the lattice displacements. Again, the fact that  $K_1$  appears constant tends to rule out this possibility also.

The change in  $\theta_0$  has prompted us to examine the sample resistance at low temperatures. The setup was similar to that used by Suits and Chen except that a carbon resistor was used as the thermometer. The absolute-temperature calibration is accurate to about  $\pm 3$  K near 40 K. The sample was suspended above a small amount of liquid helium and the resistance was monitored as the sample was warmed. The average rate of warming was about 0.08 K/min. The derivative was calculated numerically as described by Suits and Chen and is shown in Fig. 13. We see a small

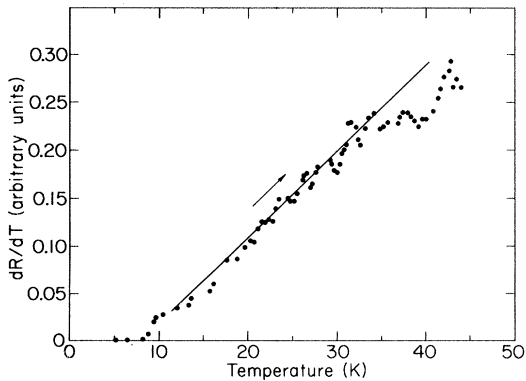


FIG. 13. Derivative of the sample resistance on warming from low temperatures. The solid line is a guide for the eye. On this scale the derivative at 70 K is 0.35.

(~10%) anomaly in the derivative between 32 and 42 K. It is tempting to associate this anomaly with the change in  $\theta_0$  seen in our NMR spectra, however, a more detailed study of this "transition" is left for future investigations.

### B. Incommensurate

In Fig. 14 we show how well the theory for the incommensurate temperature region can describe a spectrum taken at 100 K. We show the deterioration in the fit if we take the parameter  $\gamma$  to be 10 times and  $\frac{1}{10}$  times the value which gives the best fit. By considering Fig. 3 it is seen that the McMillan incommensurate state is the more proper description.

We cannot see any difference between the different types of incommensurate states which Fleming *et al.* observed on heating and cooling. This result is not unexpected on the basis of McMillan's discommensuration model. The only differences in the spectra would be due to the changes in the phase-density function  $\eta(\theta)$  caused by discommensuration crossings, which would be only a small and smeared-out part of the total signal.

The inclusion of amplitude modulation, in ad-

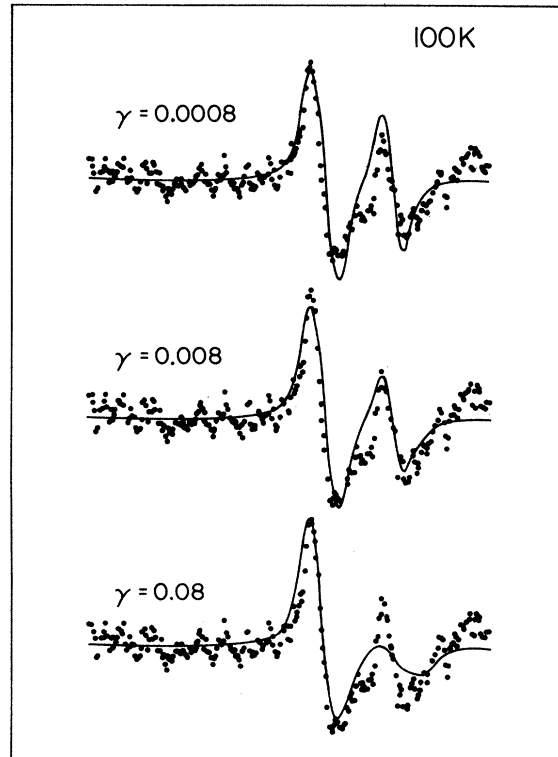


FIG. 14. Spectrum fit using McMillan's theory (center) showing the deterioration in the fit with  $\gamma \frac{1}{10}$  and 10 times the best-fit value.



dition to the phase modulation predicted by McMillan, in our line-shape model has also been pursued. We found that amplitude modulation (proportional to the phase modulation) of up to 50% did not change the resultant pseudoexperimental line shape significantly. Roughly speaking, the portion of the nuclei which are most affected by amplitude modulation contribute a small and smeared-out portion of the total signal whether or not amplitude modulation is considered—qualitatively their contribution does not change.

Since the neutron diffraction results<sup>4</sup> indicate a jump of about 10% in the CDW amplitude at 90 K, the fact that  $K_1$ , which we believe is simply related to the local CDW amplitude, does not have a large jump at the lock-in transition at 90 K is somewhat of a surprise. However, the apparent jump can also be explained by McMillan's discommensuration theory, albeit in a roundabout way, and is further evidence for the existence of discommensurations. Because of the significance of this result we will take the space to explain it in some detail. Owing to the increased ease in computation, we will restrict the mathematics to a single plane wave. The three-plane-wave case will be very similar though much more difficult to handle.

We start by writing the CDW as before,

$$\alpha(\vec{r}) = A_0 \exp[iqx + i\theta(x)]. \quad (9)$$

Presumably then,  $K_1$  is related to  $A_0$ . The square root of the neutron diffraction intensity is, however, proportional to only the lowest harmonic of this wave. That is, if we write

$$\theta(x) = \delta x + \sum_m A_m \sin(3m \delta x), \quad (10)$$

then the coefficient in front of the lowest harmonic is  $\xi A_0$ , where

$$\xi = \sum_{m_1, m_2, \dots} [J_{m_1}(A_1) J_{m_2}(A_2) \times \dots \times J_{m_n}(A_n) \times \dots] \quad (11)$$

with the condition

$$\sum_n n m_n = 0,$$

and the  $J_m$ 's are  $m$ th-order Bessel functions. If we take an approximate function for  $\theta(x)$  which is the sum of isolated discommensurations spaced  $2\Delta x$  apart,

$$\theta(x) = \frac{4}{3} \sum_n \tan^{-1} \{ \exp[\alpha(x - 2n\Delta x)] \}, \quad (12)$$

we get, after some manipulation,

$$A_n = \frac{2}{3n} \operatorname{sech} \frac{\pi^2 n}{2\alpha\Delta x}, \quad (13)$$

where  $\alpha\Delta x$  can be calculated directly to be

$$\alpha\Delta x = 2\gamma'K(\gamma')/3, \quad (14)$$

where  $K$  is a complete elliptic integral and  $\gamma' = (1 + \gamma^2)^{-1/2}$ . Using these results [Eqs. (11), (13), and (14)] we have calculated  $\xi$  as a function of  $\gamma$  numerically. For our experimental values of  $\gamma$  the series converges quite rapidly and we obtain the approximate expression  $\xi = 0.025 \log_{10}(\gamma) + 1.017$  for the range  $0.001 \leq \gamma \leq 0.1$ . For the commensurate state we have, of course,  $\xi = 1$ . At 90 K where  $\gamma$  is approximately 0.001 we get  $\xi = 0.94$ . That is, from McMillan's model and our measured values of  $\gamma$  one can expect a jump of about 6% due solely to the disappearance of the discommensurations. The effects of the hexagonal discommensuration structure shown by Nakanishi and Shiba<sup>9</sup> and the effects of amplitude modulation in the CDW discommensurate state may increase the apparent jump of 6% somewhat but we will not pursue these effects here. The curvature in the neutron results below 90 K which is also not apparent in our data may be due to the Debye-Waller factor which causes an increase in intensity as the frequency of the mode associated with the CDW increases and the temperature decreases. Thus we conclude that our results are consistent with the neutron diffraction intensity measurements of Moncton *et al.*

## VII. CONCLUSIONS

From our CW-NMR results we can conclude that the commensurate state can be characterized by three plane waves with a common phase angle at a Ta site. However, using a simple qualitative argument, we show that the phase angle is not consistent with the atomic displacements inferred by diffraction measurements and tends to support the theoretical arguments of Inglesfield<sup>6</sup> and Brouwer and Jellinek<sup>7</sup> that the displacements are in error by a minus sign. Furthermore, the phase angle seems to change between 30 and 60 K. We show that the amplitude of the CDW is roughly constant between 4 and 105 K and then appears to go to zero at about 120 K. We show that McMillan's model of the incommensurate state gives NMR line shapes which fit our data much better than the conventional theory of the incommensurate state and that the apparent jump in the CDW amplitude at the commensurate-incommensurate transition as seen by neutron diffraction can be accounted for by the disappearance of the discommensurations. That is, the commensurate regions of McMillan's incommensurate state appear to have the same wavelength, the same phase relationships, and the same amplitude as they do in the commensurate state.

## ACKNOWLEDGMENTS

We are grateful to W. L. McMillan for stimulating and helpful discussions throughout the course

of this work. This work was supported in part by the U. S. Department of Energy under Contract No. DE-AC02-76ER01198.

- 
- \*Present address: Schlumberger Well Services, P.O. Box 2175, Houston, Texas 77000.
- <sup>1</sup>J. A. Wilson, F. J. DiSalvo, and S. Mahajan, *Adv. Phys.* **24**, 117 (1975); J. A. Wilson, *Phys. Rev. B* **15**, 5748 (1977), and references therein.
- <sup>2</sup>F. J. DiSalvo, in *Electron-Phonon Interactions and Phase Transitions*, edited by T. Riste (Plenum, New York, 1977), p. 107.
- <sup>3</sup>R. M. Fleming, D. E. Moncton, D. B. McWhan, and F. J. DiSalvo, *Phys. Rev. Lett.* **45**, 576 (1980).
- <sup>4</sup>D. E. Moncton, J. D. Axe, and F. J. DiSalvo, *Phys. Rev. Lett.* **34**, 734 (1975); *Phys. Rev. B* **16**, 801 (1977).
- <sup>5</sup>J. A. Holy, M. V. Klein, W. L. McMillan, and S. F. Meyer, *Phys. Rev. Lett.* **37**, 1145 (1976); J. A. Holy, Ph.D. thesis, University of Illinois, 1977 (unpublished).
- <sup>6</sup>J. E. Inglesfield, *J. Phys. C* **13**, 17 (1980).
- <sup>7</sup>R. Brouwer and F. Jellinek, *Physica (Utrecht)* **99B**, 51 (1980).
- <sup>8</sup>W. L. McMillan, *Phys. Rev. B* **12**, 1187 (1975); **14**, 1496 (1976).
- <sup>9</sup>K. Nakanishi and H. Shibi, *J. Phys. Soc. Jpn.* **44**, 1463 (1978).
- <sup>10</sup>P. Bak, D. Mukamel, J. Villain, and K. Wentowska, *Phys. Rev. B* **19**, 1610 (1979).
- <sup>11</sup>F. C. Frank and J. H. van der Merwe, *Proc. R. Soc. London* **198**, 205 (1949).
- <sup>12</sup>A. K. Moskalev, I. A. Belobrova, and I. P. Aleksandrova, *Fiz. Tverd. Tela (Leningrad)* **20**, 3288 (1978) [*Sov. Phys.—Solid State* **20**, 1896 (1978)].
- <sup>13</sup>M. Fukui, S. Sumi, I. Hatta, and R. Abe, *Jpn. J. Appl. Phys.* **19**, L559 (1980); TSHD is defined as bis (*p*-toluene sulfonate) ester of 2,4-hexadiyne-1,6-diol.
- <sup>14</sup>A. S. Chaves, R. Gassinelli, and R. Blinc, private communication.
- <sup>15</sup>R. Blinc, S. Južnič, V. Rutar, J. Seliger, and S. Žumer, *Phys. Rev. Lett.* **44**, 609 (1980).
- <sup>16</sup>R. Blinc, private communication.
- <sup>17</sup>R. H. Friend and D. Jerome, *J. Phys. C* **12**, 1464 (1979).
- <sup>18</sup>C. Berthier, D. Jerome, and P. Molinie, *J. Phys. C* **11**, 797 (1978).
- <sup>19</sup>B. H. Suits, S. Couturié, and C. P. Slichter, *Phys. Rev. Lett.* **45**, 194 (1980).
- <sup>20</sup>C. P. Slichter, *Principles of Magnetic Resonance*, 2nd ed. (Springer, Berlin, 1978).
- <sup>21</sup>R. A. Wind and S. Emid, *J. Phys. E* **8**, 281 (1975).
- <sup>22</sup>B. H. Suits and M. C. Chen, *Phys. Lett.* **79A**, 224 (1980).
- <sup>23</sup>D. C. Abbas, T. J. Aton, and C. P. Slichter, *J. Appl. Phys.* **49**, 1540 (1978).
- <sup>24</sup>T. S. Stakelon, Ph.D. thesis, University of Illinois, 1974 (unpublished).
- <sup>25</sup>R. E. Norberg, *Phys. Rev.* **86**, 745 (1952).
- <sup>26</sup>L. Pfeiffer, M. Eibschütz, and D. Salomon, *Hyperfine Int.* **4**, 803 (1978).
- <sup>27</sup>H. N. S. Lee, M. Garcia, H. McKinzie, and A. Wold, *J. Solid State Chem.* **1**, 190 (1970).
- <sup>28</sup>G. Wexler and A. M. Woolley, *J. Phys. C* **9**, 1185 (1976).